Supporting information

Singlet Oxygen-Promoted One-Pot Synthesis of Highly Ordered Mesoporous Silica Materials via the Radical Route

Tingting Lu,[b] Wenfu Yan,[c] Guodong Feng,*[a] Xiaolin Luo,[d] Yueqiao Hu,[d] Jiale Guo,[d] Zhan Yu,[b] Zhen Zhao*[b] and Shujiang Ding*[a]

[a] Xi'an Key Laboratory of Sustainable Energy Materials Chemistry, College of Chemistry, Xi'an Jiaotong University, Xi'an 710049, People's Republic of China
[b] Institute of Catalysis for Energy and Environment, College of Chemistry and Chemical Engineering, Shenyang Normal University, Shenyang 110034, People's Republic of China
[c] State Key Laboratory of Inorganic Synthesis and Preparative Chemistry, College of Chemistry, Jilin University, Changchun 130012, People's Republic of China
[d] Key Laboratory of Advanced Molecular Engineering Materials, College of Chemistry and Chemical Engineering, Baoji University of Arts and Sciences, Baoji 721013, People's Republic of China

Corresponding Author Email:
*fengguodong00805@163.com, zhenzhao@cup.edu.cn, dingsj@mail.xjtu.edu.cn

Contents

1. Experimental section

1.1 Reagents

Tetraethyl orthosilicate (TEOS, 98%, Tianjin Fuchen Chemical Reagents Factory)

Polyethylene oxide-polypropylene oxide-polyethylene oxide triblock copolymers (P_{123}, average Mn~5800, Sigma-Aldrich Co.)

Hydrochloric acid (HCl, AR, wt.%:36.0~38.0, Beijing Chemical Works)

Ferrous sulfate heptahydrate (99%, Sinopharm Chemical Reagent Co., Ltd.)

H_2O_2 (30% (v/v), Beijing Chemical Works)

Sodium persulfate (98%, Sinopharm Chemical Reagent Co., Ltd)

5,5-Dimethylpyrroline-N-oxide (DMPO, Sigma-Aldrich Co.)

2,2,6,6-tetramethyl-4-piperidinol-N-oxyl (TMPN, Sigma-Aldrich Co.)

Ceric ammonium nitrate (CAN, Sinopharm Chemical Reagent Co., Ltd)

L-histidine (Sinopharm Chemical Reagent Co., Ltd)

Tween 60 (Sinopharm Chemical Reagent Co., Ltd)

1.2 One-pot synthesis of samples

$(NH_4)_2Ce(NO_3)_6$ system:

1 g of P_{123} was dissolved in 50 g of deionized water and TEOS (4.5 g) was mixed with a different amounts (0.005 g, 0.02 g, 0.08 g, 0.1 g, 0.16 g, 0.2 g) of $(NH_4)_2Ce(NO_3)_6$. The mixture was stirred vigorously for 24 h at 313 K (precursor) and then was transferred into an autoclave, aged for 72 h at 373 K. The resultant solid was filtered, washed, and dried at 333 K for 15 h. After calcined at 823 K for 10 h, the samples1-6 were obtained.

0.78 g of Tween 60 was dissolved in 50 g of deionized water and TEOS (1.43 g) was mixed with a trace amount (0.0125 g) of $(NH_4)_2Ce(NO_3)_6$. The mixture was stirred vigorously for 24 h at 318 K (precursor) and then was transferred into an autoclave, aged for 24 h at 373 K. The resultant solid was filtered, washed, and dried at 333 K for 15 h. After calcined at 823 K for 10 h, the sample 9 was obtained.

Fenton reagents system:

1 g of P_{123} was dissolved in 50 g of deionized water and TEOS (4.5 g) was mixed with a trace amount (0.01 g) of $FeSO_4 \cdot 7H_2O$ and 300μL 30wt%H_2O_2. The mixture was stirred vigorously for 24 h at 313 K (precursor) and then was transferred into an autoclave, aged for 72 h at 373 K. The resultant solid was filtered, washed, and dried at 333 K for 15 h.

After calcined at 823 K for 10 h, the sample 7 (Fe-SBA-15) was obtained.

0.78 g of Tween 60 was dissolved in 50 g of deionized water and TEOS (1.43 g) was mixed with a trace amount (0.02 g) of $FeSO_4 \cdot 7H_2O$ and 300 μL 30 wt% H_2O_2. The mixture was stirred vigorously for 24 h at 318 K (precursor) and then was transferred into an autoclave, aged for 24 h at 373 K. The resultant solid was filtered, washed, and dried at 333 K for 15 h. After calcined at 823 K for 10 h, the sample 10 was obtained.

$Na_2S_2O_8$ system:

1 g of P_{123} was dissolved in 50 g of deionized water and TEOS (4.5 g) was mixed with a trace amount (0.0087 g) of $Na_2S_2O_8$. The mixture was stirred vigorously for 24 h at 313 K (precursor) and then was transferred into an autoclave, aged for 72 h at 373 K. The resultant solid was filtered, washed, and dried at 333 K for 15 h. After calcined at 823 K for 10 h, the sample 8 (disordered structure material) was obtained.

1.3 Release experiment

Ce-SBA-15: 10 ml of 20% hydrochloric acid was added to 0.2 g of Ce-SBA-15 sample and stirred at room temperature for 5 minutes. After that, the sample was centrifuged and dried. ICP and small angle XRD detection were used to compare the difference between the acquired sample and the original Ce-SBA-15 sample.

Fe-SBA-15: 10 ml of 20% hydrochloric acid was added to 0.2 g of Fe-SBA-15 sample and stirred at room temperature for 5 minutes. After that, the sample was centrifuged and dried. ICP and small angle XRD detection were used to compare the difference between the acquired sample and the original Fe-SBA-15 sample.

1.4 Calculation of samples yields

The yields were calculated by the formula below based on the SiO_2:

$$\text{Yield} = \frac{\text{Weight of calcined sample}}{\text{Theoretical weight of SBA-15/MSU-4}}$$

The theoretical weight of SBA-15/MSU-4 was calculated according to the mole of SiO_2 from TEOS.

1.5 Theoretical calculation

In this work, we used Gaussian 16 software[1] for all calculations within the framework of DFT. All the molecular structures were computed with the B3LYP (Becke, three-parameter, Lee-Yang-Parr) hybrid functional[2] to describe the exchange–

correlation energies. Basis sets were employed for high-level B3LYP calculations at 6-31+G(d,p) was adopted for atoms including C, O, Si, and H [3]. Vibrational frequency calculations were performed on all minima states, and each minimum was identified to have no imaginary frequencies.

The reaction pathway is as follow: TEOS interacts with the $^1O_2$ leading to a Gibbs free energy of 3.35 kcal/mol. The first transition states ascribed by formation of OOH group for $^1O_2$ via obtaining a H atom from the CH_2 group. The second transition state is contributed by formation of OH and CH_3CHO-O-Si group (dissociation of O-O bond in the OOH). The C atom only bonded with the O atom obtains the H atom, forming CH_3COOH. The OH group interacts with the Si atom, leading to the final products. The rate-determining step is break of the O-O bond.

2. Characterizations

XRD patterns were recorded on a Bruker D8 Advance diffractometer using Cu Kα radiation (λ = 1.5406 Å) (40 kV and 40 mA) over the range 0.5-5°. By means of a JEM-2100Plus (JEOL, Japan) instrument, transmission electron microscopic (TEM) images of the samples were obtained. The Scanning electron micrographs (SEM) were taken on HITACHI UHR FE-SEM SU8010 electron microscope. Nitrogen adsorption/desorption measurements were carried out on a McKesson ASAP-2460 analyzer at 77.2 K after the samples were degassed at 350 °C under vacuum. The pore size distribution curves were calculated from the analysis of desorption branch of the isotherm by the BJH (Barrett-Joyner-Halenda) method. The Fe concentration in solution was measured by an inductively coupled plasma (ICP) emission spectrometer (Prodigy).

All MS measurements were carried out on a quadrupole time-of-flight (Q-TOF) mass spectrometer (6545B, Agilent Technologies, USA). The original ESI source was removed and the interlock was overridden. A typical DC high voltage of 2.7 kV was applied between the PESI probe and the ion sampling orifice of the mass spectrometer for electrospraying. Full-scan positive ion spectra were acquired and processed using the default Mass Hunter Workstation package. The capillary temperature was maintained at 275 °C. The dry gas flow rate was set to 2 L min^{-1}. The fragmentor voltage, skimmer voltage and oct rf V_{pp} voltage were set at 60, 10 and 400 V, respectively. The collision voltage was adjusted at 0 V to avoid the generation of in-source fragmentation products which might be misinterpreted to be degradation products of the precursor.

The EPR spectra were recorded on a Brookhaven FA300 EPR spectrometer equipped with a UV lamp (center wave length: 365nm). The detailed instrumental parameters were as follows: scanning frequency: 9.8 GHz; central field: 3510 G; scanning width: 100 G; scanning power: 6 mW; scanning temperature: 293 K.

DMPO trappings are shown in the following reaction:

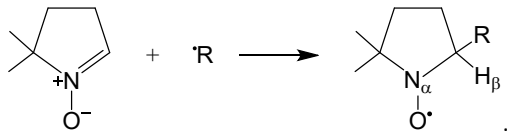

The hyperfine coupling constants (*hfcs*) of the nitrogen and β-proton (a_N and $a_{H\beta}$) were given in the main text when referred.

Detection of •OH/DMPO:

200 μL of initial reaction mixture was added into 200 μL of aqueous DMPO solution with the concentration of 80 mM. The mixture was shaken by hand for 1 minute and transferred into a quartz cell. Then, the solution was transferred into an aqueous cell and the EPR data collection was started.

TMPN trappings are shown in the following reaction:

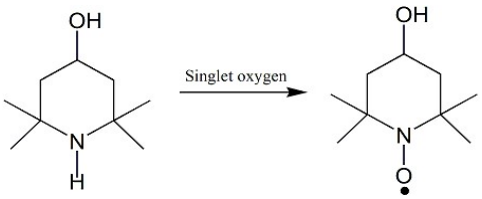

Detection of $^1O_2$/TMPN:

200 μL of initial reaction mixture was added into 200 μL of aqueous TMPN solution with the concentration of 80 mM. The mixture was shaken by hand for 1 minute and transferred into a quartz cell. Then, the solution was transferred into an aqueous cell and the EPR data collection was started.

Ref:

[1]. M. J. Frisch, G. W. Trucks, H. B. Schlegel, G. E. Scuseria, M. A. Robb, J. R. Cheeseman, G. Scalmani, V. Barone, G. A. Petersson, H. Nakatsuji, X. Li, M. Caricato, A. V. Marenich, J. Bloino, B. G. Janesko, R. Gomperts, B. Mennucci, H. P. Hratchian, J. V. Ortiz, A. F. Izmaylov, J. L. Sonnenberg, D. Williams-Young, F. Ding, F. Lipparini, F. Egidi, J. Goings, B. Peng, A. Petrone, T. Henderson, D. Ranasinghe, V. G. Zakrzewski, J. Gao, N. Rega, G. Zheng, W. Liang, M. Hada, M. Ehara, K. Toyota, R. Fukuda, J. Hasegawa, M. Ishida, T. Nakajima, Y. Honda, O. Kitao, H. Nakai, T. Vreven, K. Throssell, J. A.

Montgomery, Jr., J. E. Peralta, F. Ogliaro, M. J. Bearpark, J. J. Heyd, E. N. Brothers, K. N. Kudin, V. N. Staroverov, T. A. Keith, R. Kobayashi, J. Normand, K. Raghavachari, A. P. Rendell, J. C. Burant, S. S. Iyengar, J. Tomasi, M. Cossi, J. M. Millam, M. Klene, C. Adamo, R. Cammi, J. W. Ochterski, R. L. Martin, K. Morokuma, O. Farkas, J. B. Foresman, and D. J. Fox, Gaussian, Inc., Wallingford CT, 2016.

[2]. F. J. Devlin, J. W. Finley, P. J. Stephens and M. J. Frisch, Ab Initio Calculation of Vibrational Absorption and Circular Dichroism Spectra Using Density Functional Force Fields: A Comparison of Local, Nonlocal, and Hybrid Density Functionals. J. Phys. Chem. 1995, 99, 16883-16902, DOI: 10.1021/j100046a014

[3]. A. D. McLean and G. S. Chandler, Contracted Gaussian basis sets for molecular calculations. I. Second row atoms, Z=11-18. J. Chem. Phys. 1980, 72, 5639-5648, DOI: 10.1063/1.438980

3. Supplementary Figures and Table

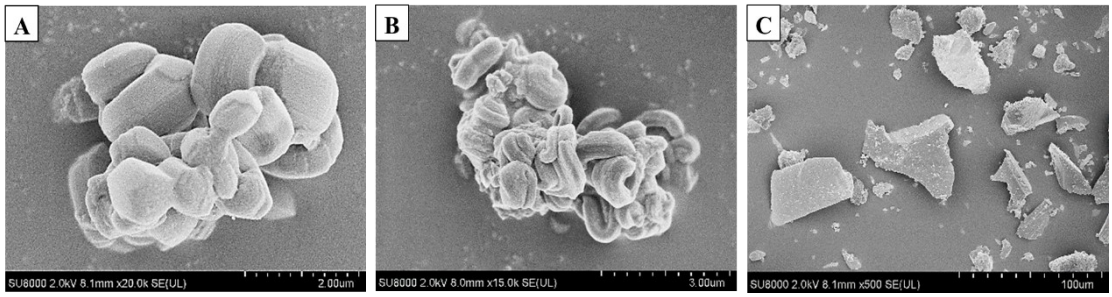

Fig. S1 SEM images of the samples one-pot synthesized without addition of acid by adding $(NH_4)_2Ce(NO_3)_6$ (A), adding the Fenton reagent (B), and adding $Na_2S_2O_8$ (C)

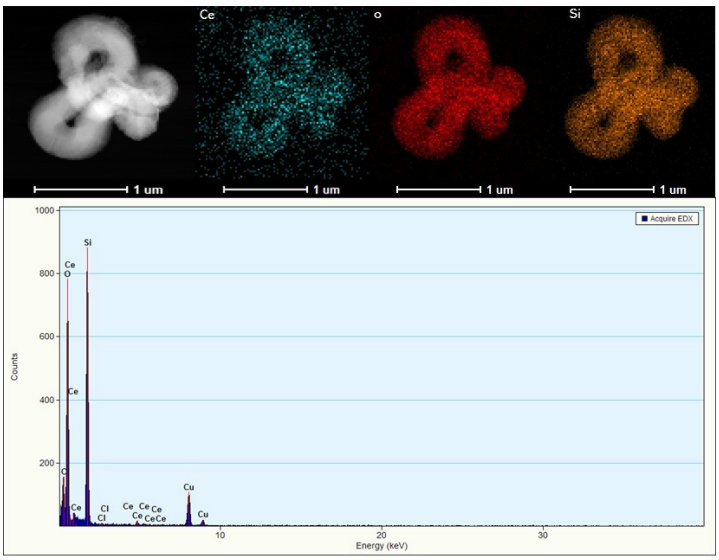

Fig. S2 TEM image and EDS mapping (Ce: Cyan, O: red, Si: orange) of the Ce-SBA-15 sample synthesized by the one-pot route

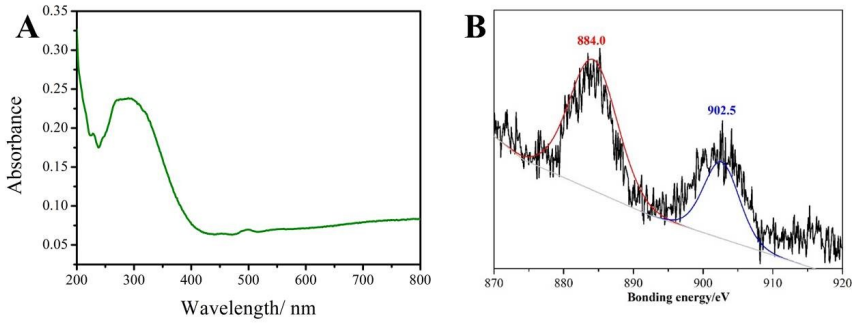

Fig. S3 UV-vis spectra (A) and Ce 3d XPS spectra (B) of the Ce-SBA-15 sample synthesized by the one-pot route

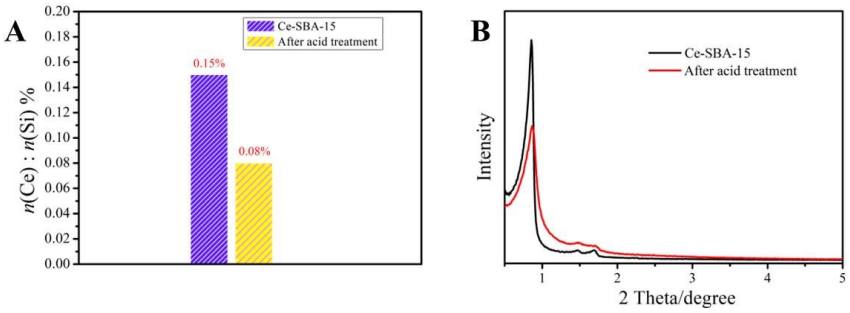

Fig. S4 The Ce/Si molar ratio (A) and XRD patterns (B) of the as-synthesized Ce-SBA-15 sample and acid-treated Ce-SBA-15 sample

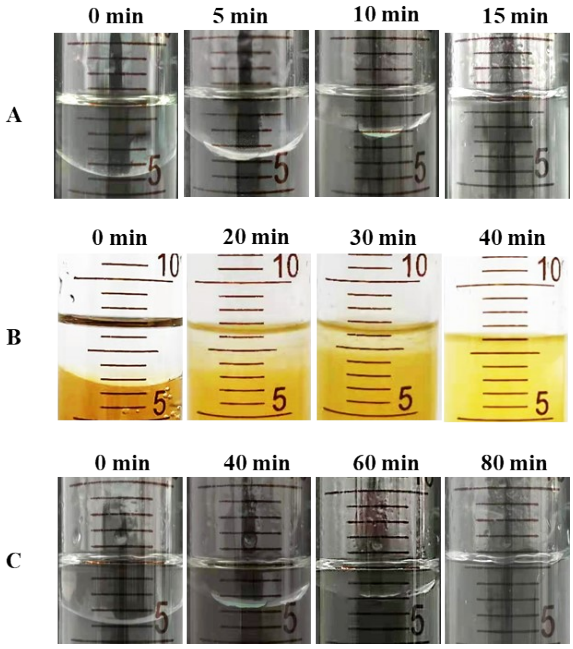

Fig. S5 The images of TEOS hydrolysed by adding $(NH_4)_2Ce(NO_3)_6$ (A), Fenton reagent (B), and $Na_2S_2O_8$ (C) at different time under the same conditions

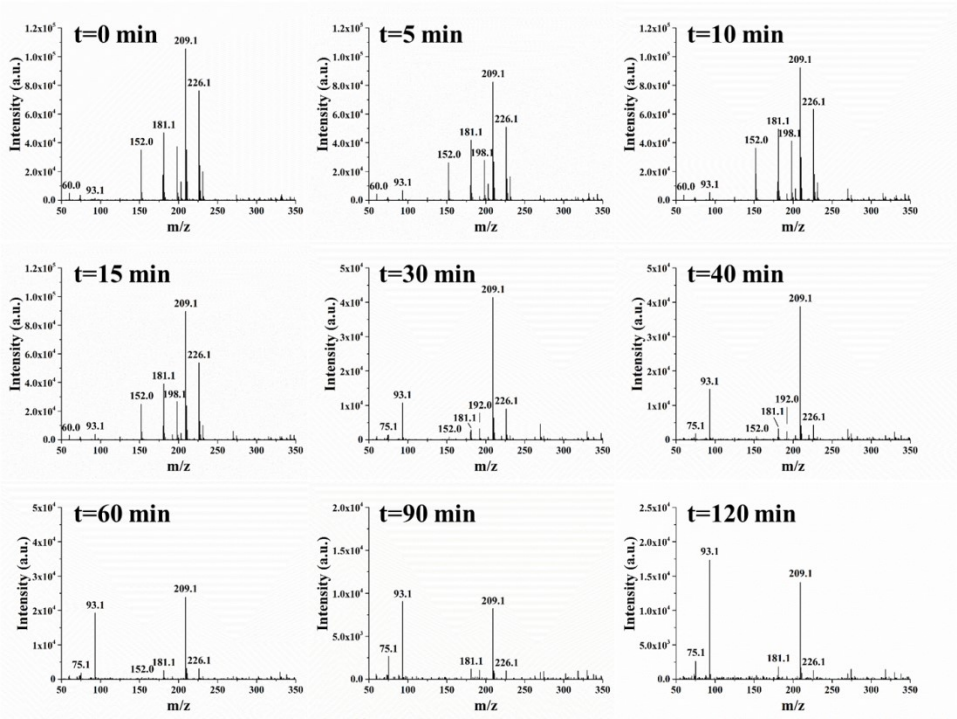

Fig. S6 Time-resolved PESI-MS results of the hydrolysis reaction of TEOS promoted by $(NH_4)_2Ce(NO_3)_6$

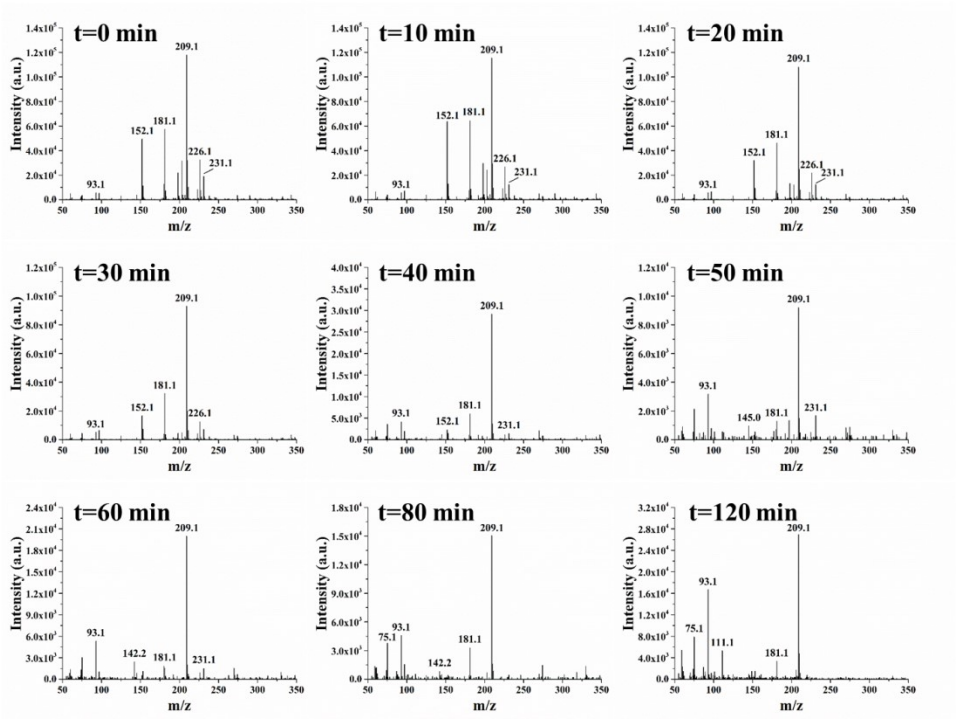

Fig. S7 Time-resolved PESI-MS results of the hydrolysis reaction of TEOS promoted by 2 mol/L HCl

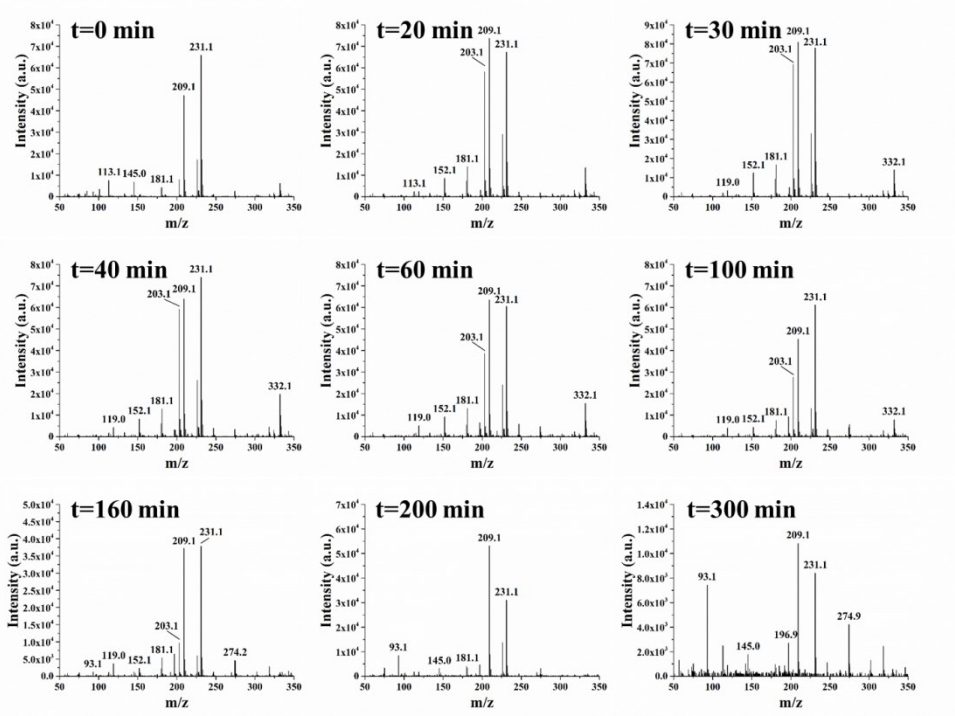

Fig. S8 Time-resolved PESI-MS results of the hydrolysis reaction of TEOS promoted by $Na_2S_2O_8$

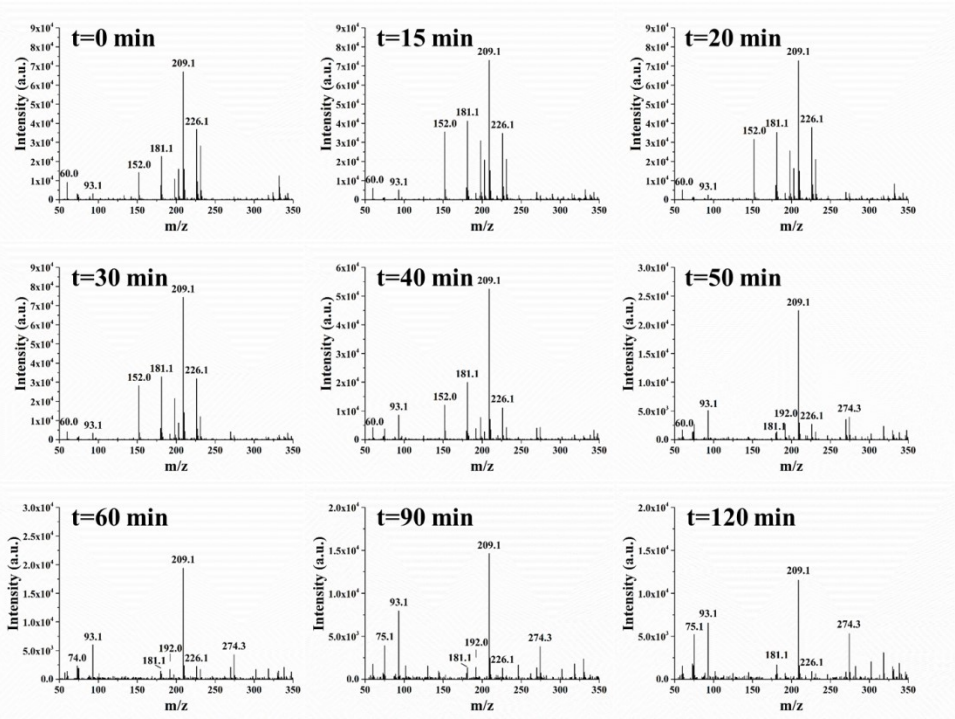

Fig. S9 Time-resolved PESI-MS results of the hydrolysis reaction of TEOS promoted by the Fenton reagent

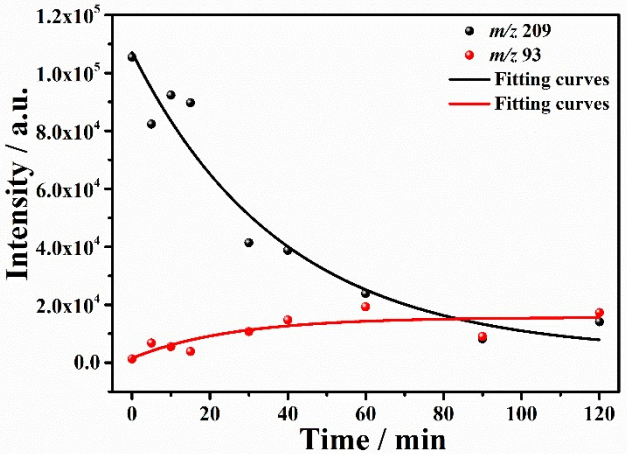

Fig. S10 Intensity of the ion at *m/z* 209 (black) and *m/z* 93 (red) as a function of time in the hydrolysis reaction promoted by $(NH_4)_2Ce(NO_3)_6$

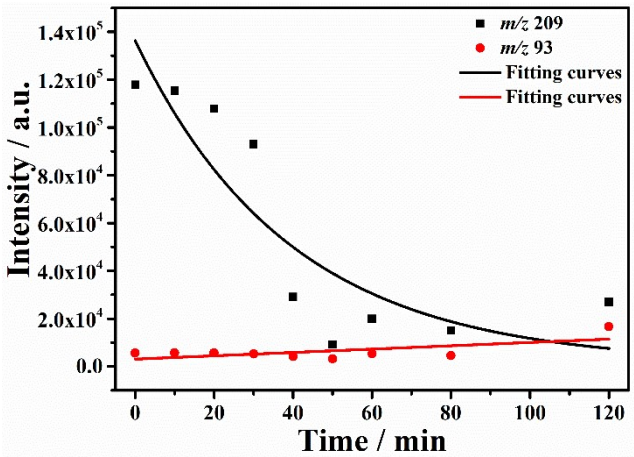

Fig. S11 Intensity of the ion at *m/z* 209 (black) and *m/z* 93 (red) as a function of time in the hydrolysis reaction promoted by 2 mol/L HCl

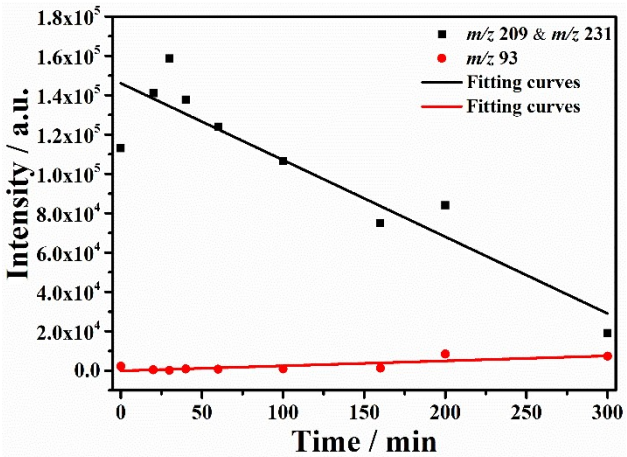

Fig. S12 Intensity of the ion at *m/z* 209, *m/z* 231 (black) and *m/z* 93 (red) as a function of time in the hydrolysis reaction promoted by $Na_2S_2O_8$

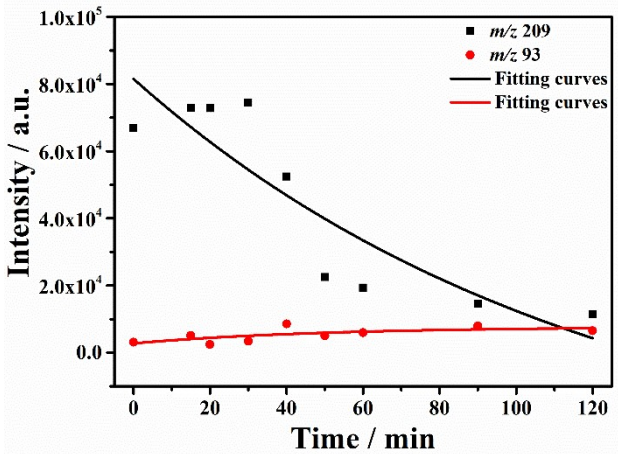

Fig. S13 Intensity of the ion at *m/z* 209 (black) and *m/z* 93 (red) as a function of time in the hydrolysis reaction promoted by Fenton reagent

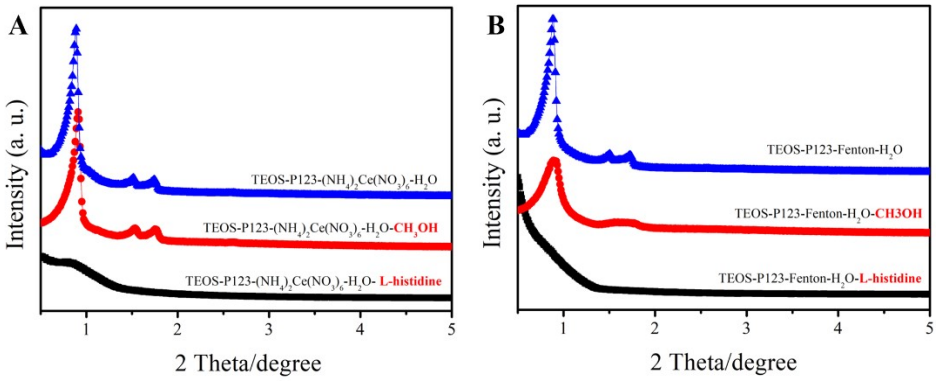

Fig. S14 XRD patterns of the samples one-pot synthesized in the $(NH_4)_2Ce(NO_3)_6$ system (A) and Fenton reagent system (B) with the addition of H_2O (blue), CH_3OH (red), and L-histidine (black)

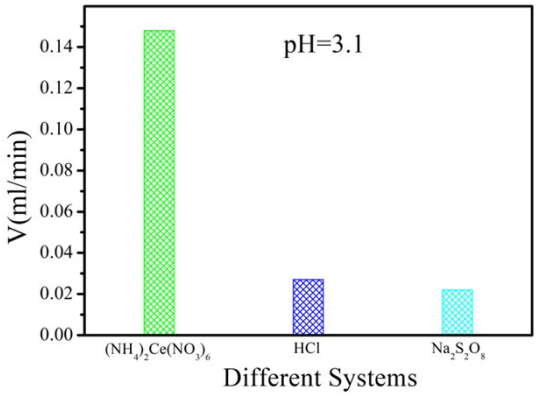

Fig. S15 The hydrolysis rate of TEOS in different system at identical pH value of 3.1

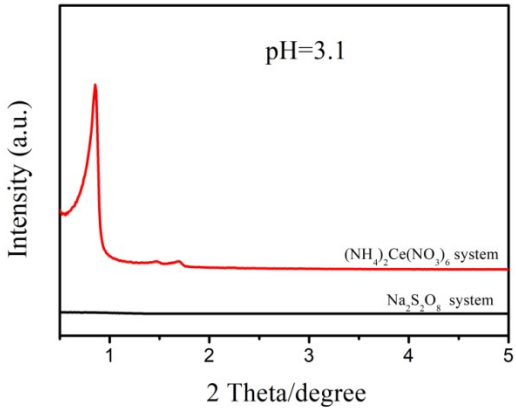

Fig. S16 XRD patterns of the samples one-pot synthesized in the $(NH_4)_2Ce(NO_3)_6$ system and $Na_2S_2O_8$ system at identical pH value of 3.1

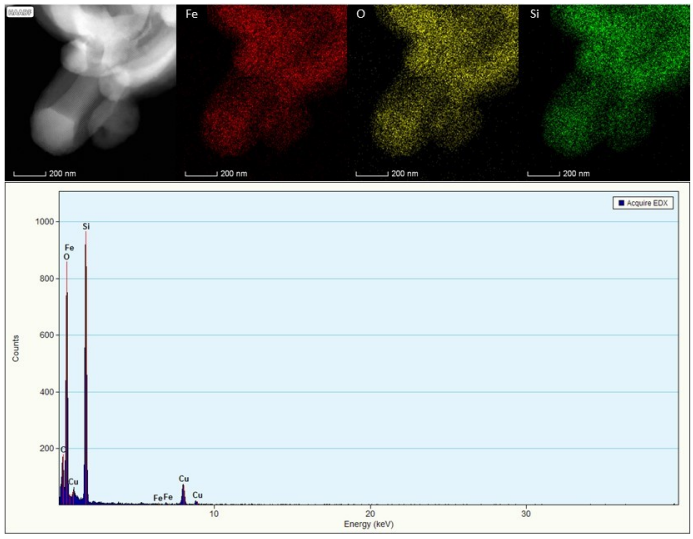

Fig. S17 The TEM image and EDS mapping (Fe: red, O: yellow, Si: green) of the Fe-SBA-15 sample synthesized by the one-pot route

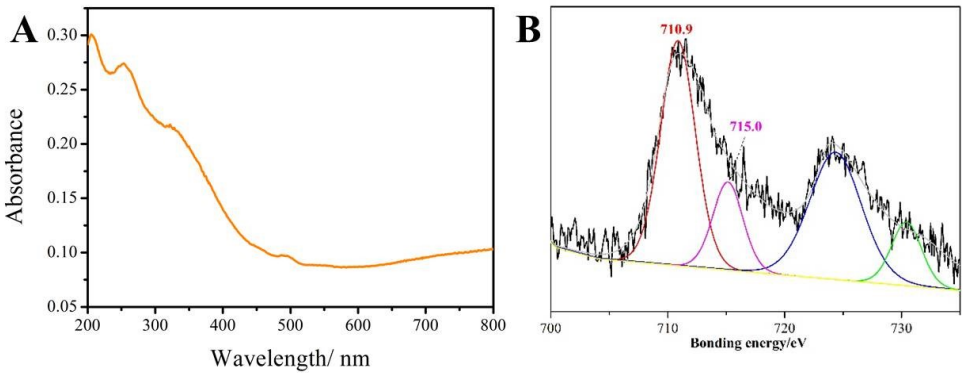

Fig. S18 UV-vis spectra (A) and Fe 2p XPS spectra (B) of the Fe-SBA-15 sample synthesized by the one-pot route

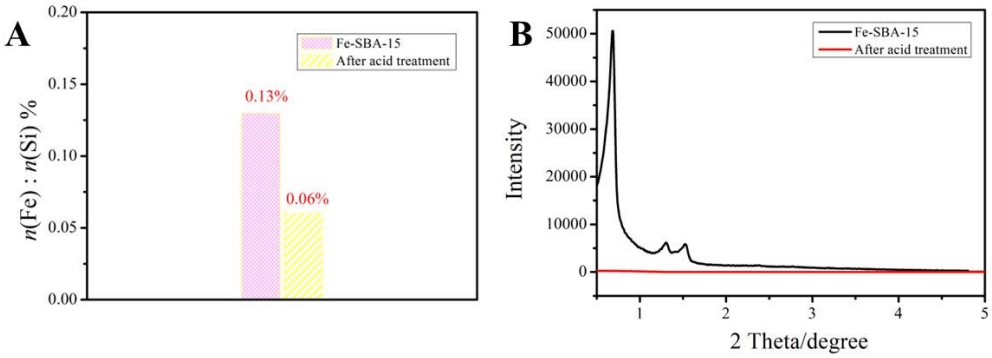

Fig. S19 The Fe/Si molar ratio (A) and XRD patterns (B) of the as-synthesized Fe-SBA-15 sample and acid-treated Ce-SBA-15 sample

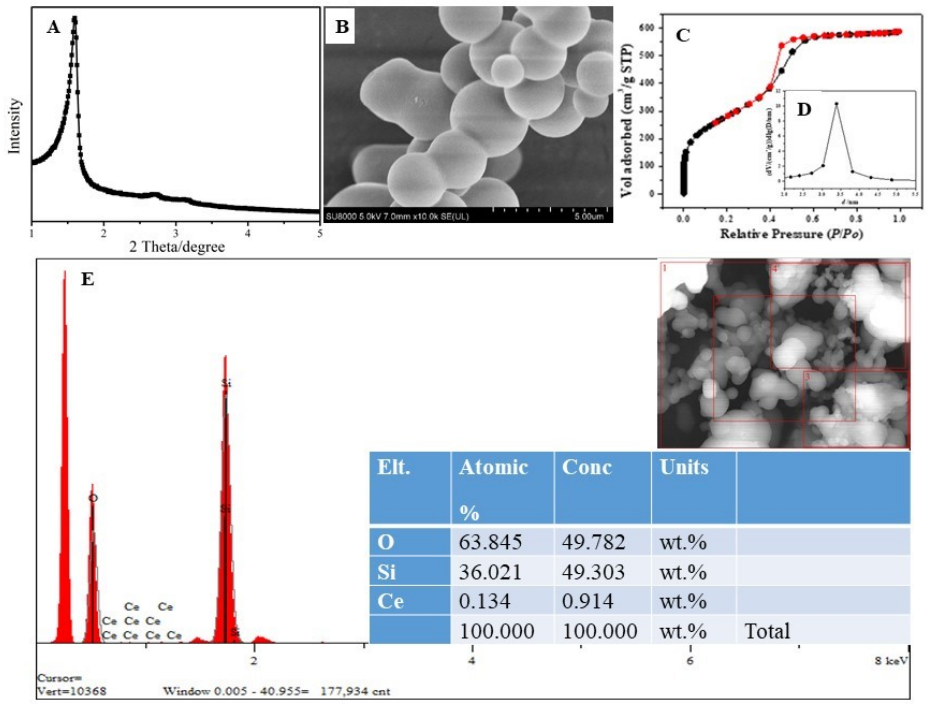

Elt.	Atomic %	Conc	Units	
O	63.845	49.782	wt.%	
Si	36.021	49.303	wt.%	
Ce	0.134	0.914	wt.%	
	100.000	100.000	wt.%	Total

Fig. S20 The low-angle XRD pattern (A), SEM image (B), nitrogen adsorption-desorption isotherm (C) and the pore size distribution (D) and EDS mapping (E) of the MSU-4 materials one-pot synthesized in the $(NH_4)_2Ce(NO_3)_6$ system

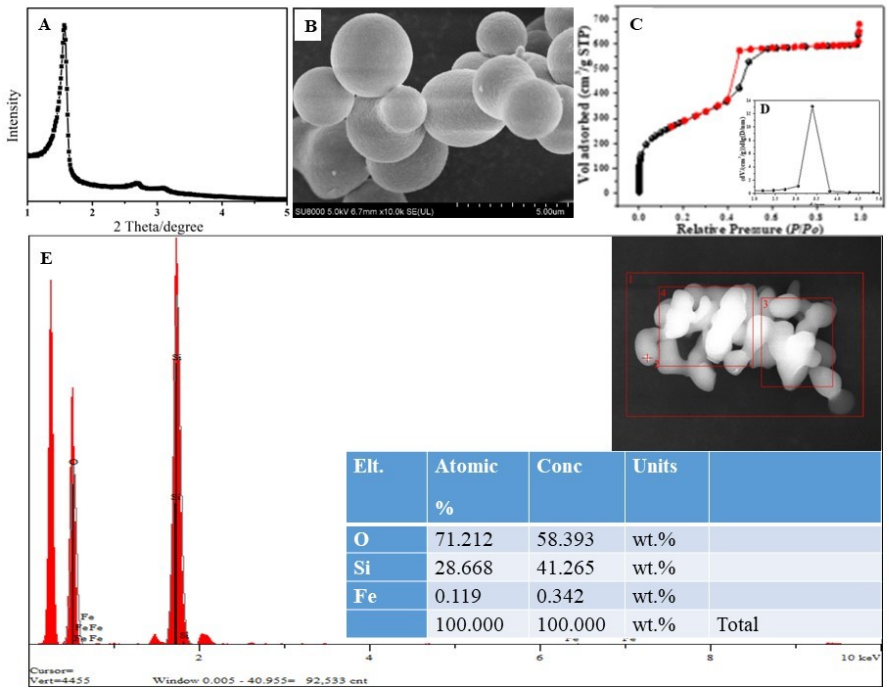

Elt.	Atomic %	Conc	Units	
O	71.212	58.393	wt.%	
Si	28.668	41.265	wt.%	
Fe	0.119	0.342	wt.%	
	100.000	100.000	wt.%	Total

Fig. S21 The low-angle XRD pattern (A), SEM image (B), nitrogen adsorption-desorption isotherm (C), the pore size distribution (D), and EDS mapping (E) of the MSU-4 materials one-pot synthesized in the Fenton reagent system

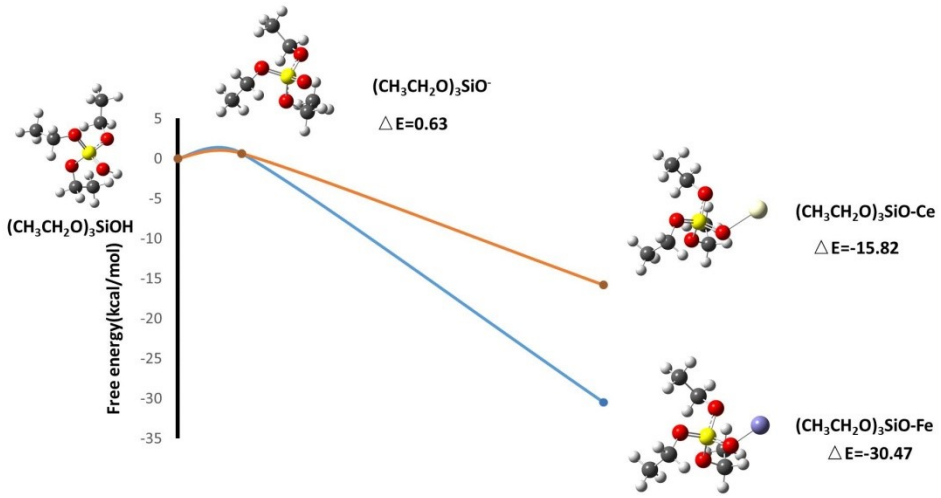

Fig. S22 Gibbs free energy profile and optimized geometry of the structures involved in the incorporation of Ce and/or Fe within the mesoporous silica materials

Table S1. Physicochemical properties of calcined samples prepared using different methods

Sam	Reaction system	Initiator		Products	Metal /Si molar ratio[a] (%)	d^b (nm)	S_{BET} (m^2g^{-1})	Pore volume (cm^3g^{-1})	Pore diameter[c] (nm)	Wall thickness[d] (nm)	Yield (%)
1	**TEOS-P_{123}-$(NH_4)_2Ce(NO_3)_6$-H_2O**	$(NH_4)_2Ce(NO_3)_6$/ mmol	0.009	Ce-SBA-15	-	10.3	447	1.37	9.4	2.4	36
2			0.036	Ce-SBA-15	0.15	9.9	978	0.98	6.2	5.2	91
3			0.144	Ce-SBA-15	-	10.1	879	0.87	5.8	5.9	85
4			0.182	Ce-SBA-15	-	9.2					85
5			0.29	Ce-SBA-15	-	9.8	748	0.5	4.9	6.4	72
6			0.36	Ce-SBA-15	-	9.5					60
7	**TEOS-P_{123}-Fenton-H_2O**	300μL 30wt%H_2O_2+ $FeSO_4 \cdot 7H_2O$/ mmol	0.036	Fe-SBA-15	0.13	10.1	983	0.967	6.06	5.6	95
8	**TEOS-P_{123}-$Na_2S_2O_8$-H_2O**	$Na_2S_2O_8$/ mmol	0.036	-	-		-	-	-	-	-
9	**TEOS-Tween60-$(NH_4)_2Ce(NO_3)_6$-H_2O**	$(NH_4)_2Ce(NO_3)_6$/ mmol	0.036	Ce-MSU-4	0.28	5.53	1020	0.895	3.26	3.13	86
10	**TEOS-Tween 60-Fenton-H_2O**	300μL 30wt% H_2O_2+$FeSO_4 \cdot 7H_2O$/ mmol	0.072	Fe-MSU-4	0.36	5.64	1038	1.016	3.77	2.74	84

[a]The Metal/Si ratios in the calcined materials were calculated by the ICPAES method. [b]$d_{(100)}$ spacing or d value of characteristic reflection of the as-synthesized products after calcination at 550 °C for 6 h. [c]The pore diameters were calculated by the desorption branch of the isotherms according the BJH method. [d]Calculated by a^0 - pore size ($a^0 = 2d_{(100)} / 3^{1/2}$)